A Robust Cubature Kalman Filter for GPS Vector Tracking Loop

Boya Zhang, Shuai Chen, Xiaohan Zhu

***Abstract*—Vector Tracking Loop (VTL) is a recently proposed method to enhance GPS receiver performance. In VTL, a center navigation filter usually a Kalman filter (KF) is utilized to estimate navigation solutions and complete signal tracking together. Thus, all channels are processed together and mutual aiding can be obtained. Compared with Scalar Tracking Loop (STL), in which signal tracking is operated independently, researches have demonstrated that VTL performs better signal tracking performance. However, the nonlinear problems or the measurement outliers might affect the navigation filter and hinder VTL performance. This paper investigates applying robust adaptive cubature Kalman filter (AR-CKF) to VTL navigation filter. Robust M estimation is employed to resistant the measurement outliers and an adaptive factor is utilized to address the dynamic disturbance errors. A 3D dynamic trajectory is generated to test the AR-CKF based VTL. Simulations are implemented in a VTL software receiver, the results from comparing a common Kalman Filter with AR-CKF, which demonstrates that the employed AR-CKF improves VTL stability and accuracy.**

***Index Terms*—Cubature Kalman Filter,Vector Tracking Loop,M estimation,GPS,Measurement Outliers**

I. INTRODUCTION

Global Navigation Satellite System (GNSS) is a satellite based navigation system which is widely employed in civil and military applications, especially Global Positioning System (GPS). Users with a GPS receiver available to the Line-Of-Sight (LOS) satellites signal are able to obtain position, navigation and timing (PNT) information [1-2]. At the moment, there are two major GPS receivers' architectures termed as Scalar Tracking Loop (STL) and Vector Tracking Loop (VTL) [20-21].

In a STL, the tracking loops are employed to estimate the pseudo-range and pseudo-range rate measurements of the available satellites. In which, a delay lock loop (DLL) is generally used to estimate the pseudo-range and a frequency lock loop (FLL) or a phase lock loop (PLL) is commonly used to estimate the pseudo-range rate. Navigation solutions are determined by using an iterative least square algorithm, a conventional Kalman filter, EKF, UKF and other modified Kalman filters [3][21]. In this architecture, pseudo-ranges and pseudo-range rates from all the tracking channels are independent [4-5]. However, it can be seen that all the channels share the common navigation solutions, which might be fed back to aid signal tracking

VTL is a recently proposed signal tracking architecture, which performs signal tracking of all channels together using a center navigation filter. The VTL is firstly initialized by Spilker for enhancing weak signals tracking [4]. Starting from this, various types of VTL implementation has been investigated. Lashley presents a Vector Delay/Frequency Lock Loop (VDLL/FLL) including thermal noise performance analysis using the rule of thumb tracking thresholds [5]. In this work, VTL and STL comparison is carried out and the improvements of VTL in signal tracking are quantified [6]. Then, T Pany describes an implementation of VDLL/VFLL in a GPS receiver, which is utilized to analyze signal power strength of GPS C/A code with two different C/N0 estimators. Results show that the receiver is able to estimate GPS C/A code signals power even the signal power strength is below 10dB/Hz [7]. In dynamic signal tracking, the results show the VTL can operate in the situation with signal power of 19dB-Hz through 2g, 4g, and 8g coordinates turns [7]. Apart from signal tracking capacity improving, VTL has the ability to bridge signal outages and work with providing moderate navigation solutions in short time with the amount of the available satellites fading below 4 [4-9]. Specifically, Changhui Jiang investigates a Chip Scale Atomic Clock (CSAC) based VTL, and the results show that positioning accuracy especially altitude accuracy can be improved with the precise time from CSAC [20].

Over the recent years, there are two major approaches to enhance VTL performance. Firstly, broad interests are attracted to tracking models modification. Luo proposes a double filter model for VTL computation efficiency [10]. Wu investigates a new non-coherent VTL and its application in integration with the Inertial Navigation System (INS) [11]. Besides the VTL model modification, researchers are dedicated to the navigation filter enhancement for addressing nonlinearity problem and noise suppression. In VTL, the navigation filter is commonly a Extended Kalman Filter (EKF), which is an estimator which is built by the first order linearization of the nonlinear model. It may suffer from the performance degradation or divergence problem, since linearization processing will cause the model miss-matching [12-14]. To better address the nonlinearity, unscented Kalman filter (UKF) is proposed. In UKF, a number of sigma points are used to propagate the probability of state distribution through the nonlinear dynamics of system not the first order linearization in EKF [12-15]. However, the rounding errors of numerical calculation for UKF may

Boya Zhang, School of Automation, Nanjing University of Science and Technology, Nanjing,China.

Shuai Chen, School of Automation, Nanjing University of Science and Technology, Nanjing,China.

Xiaohan Zhu, School of Automation, Nanjing University of Science and Technology, Nanjing,China.

This work was supported by the Fundamental Research Funds of the Central University(No. 30917011105) and Defense Basic Research Plan(No.JCKY2016606B004).This work also got the special grade of the financial support from the China Postdoctoral Science Foundation (No. 2016T90461).

destroy the non-negative and asymmetry of covariance matrix, therefore, the convergence rate of the UKF approach is slow and the system may also be unstable. Newly, Cubature Kalman Filter (CKF) is proposed to realize nonlinear estimation. Compared with UKF, a new transformation rule termed as third-degree spherical-radial cubature is employed in CKF as opposed to the UT in UKF approach. With new transformation rule, the performance can be improved in terms of accuracy, numerical stability [14-18].

In this paper, CKF is employed to solve this nonlinear estimation problem. Additionally, the robust M estimation to adaptively adjust the cubature Kalman filter measurement noise matrix to address the measurement outliners and noise uncertainty. The adaptive robust CKF (ARCKF) is employed as the navigation filter to enhance the estimation performance and signal tracking.

II. NONLINEAR MODEL OF VECTOR TRACKING LOOP

Figure 1 shows the working flow of a typical VTL based VDLL and VFLL. Navigation filter estimated the state errors utilizing observation data from scaled carrier and code discriminators outputs. Then the estimated state errors are fed back to tracking loop for generating local signal replica. The correlator mixed the local signal replica and the incoming immediate frequency signal (IF) to provide navigation filter observation data. Thereby, the signal tracking and the navigation determination are accomplished together through a single navigation filter. Remainder of this section gives the mathematical model of VTL in detail.

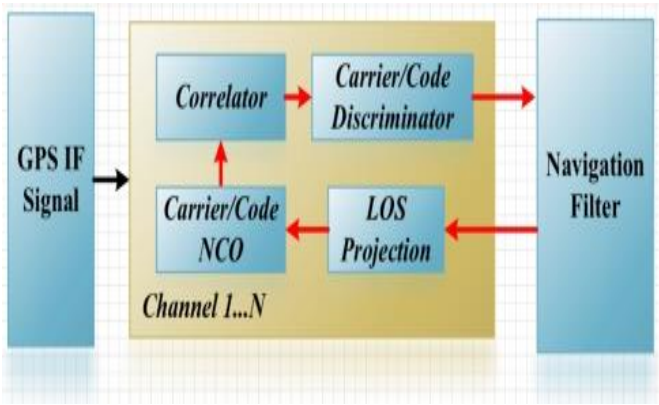

Figure 1. A typical VTL working flow

A. State Equation

The navigation filter states commonly includes position error, velocity error and time bias/drift. The deviation details of this model can be seen in references [20-22]:

$$\delta \boldsymbol{X} = \begin{bmatrix} \delta \boldsymbol{P}_{3\times1} \\ \delta \boldsymbol{V}_{3\times1} \\ \delta \boldsymbol{B}_{2\times1} \end{bmatrix} = \begin{bmatrix} \boldsymbol{Pos\ Error} \\ \boldsymbol{Vel\ Error} \\ \boldsymbol{Clk\ Error} \end{bmatrix} \tag{1}$$

The state equation can be written as equation (2):

$$\begin{bmatrix} \delta x_k \\ \delta v_{x,k} \\ \delta y_k \\ \delta v_{y,k} \\ \delta z_k \\ \delta v_{z,k} \\ c\cdot\delta t_{b,k} \\ c\cdot\delta t_{d,k} \end{bmatrix} = \begin{bmatrix} 0 & T & 0 & 0 & 0 & 0 & 0 & 0 \\ 0 & 0 & 0 & 0 & 0 & 0 & 0 & 0 \\ 0 & 0 & 0 & T & 0 & 0 & 0 & 0 \\ 0 & 0 & 0 & 0 & 0 & 0 & 0 & 0 \\ 0 & 0 & 0 & 0 & 0 & T & 0 & 0 \\ 0 & 0 & 0 & 0 & 0 & 0 & 0 & 0 \\ 0 & 0 & 0 & 0 & 0 & 0 & 1 & T \\ 0 & 0 & 0 & 0 & 0 & 0 & 0 & 0 \end{bmatrix} \begin{bmatrix} \delta x_{k-1} \\ \delta v_{x,k-1} \\ \delta y_{k-1} \\ \delta v_{y,k-1} \\ \delta z_{k-1} \\ \delta v_{z,k-1} \\ c\cdot\delta t_{b,k-1} \\ c\cdot\delta t_{d,k-1} \end{bmatrix} + \begin{bmatrix} \omega_x \\ \omega_{vx} \\ \omega_y \\ \omega_{vx} \\ \omega_z \\ \omega_{vz} \\ \omega_b \\ \omega_d \end{bmatrix} \tag{2}$$

The model is constructed in ECEF coordinates. Thereby, δx_k , δy_k , δz_k : User position error in ECEF frame at k_{th} time epoch; δx_{k-1} , δy_{k-1} , δz_{k-1} : User position error in ECEF frame at the $(k-1)_{th}$ time epoch; $\delta v_{x,k}$, $\delta v_{y,k}$, $\delta v_{z,k}$: User velocity error in ECEF frame at the k_{th} time epoch; $\delta v_{x,k-1}$, $\delta v_{y,k-1}$, $\delta v_{z,k-1}$: User velocity error in ECEF frame at the $(k-1)_{th}$ time epoch; $c\cdot\delta t_{b,k}$, $c\cdot\delta t_{b,k-1}$: User clock bias at the k_{th} and $(k-1)_{th}$ time epoch respectively; $c\cdot\delta t_{d,k}$, $c\cdot\delta t_{d,k-1}$: User clock drift at the k_{th} and $(k-1)_{th}$ time epoch respectively; ω_x , ω_y , ω_z : Position error noise; ω_{vx} , ω_{vy} , ω_{vz} : Velocity error noise; ω_b , ω_d :Clock bias error noise, clock drift error noise; c :The speed of the light in vacuum; T :The integration time (1 ms).

B. Measurement Equation

The measurement equation is constructed on the mathematical model between discriminators outputs (code phase errors and carrier frequency errors) and the navigation filter state variables. The relationship between position error and code phase error [9-10]:

$$\varphi^j_{code,k} = \Delta \boldsymbol{P}_k \cdot \boldsymbol{H}_{j,k} + c\cdot t_{b,k} + \omega_{j,k} \tag{3}$$

Where, the $\varphi^j_{code,k}$ is the code phase error, $\Delta \boldsymbol{P}_k$ is the position error in ECEF coordinates, c is the light speed addressed as a constant value, $t_{b,k}$ is the clock bias, the $\omega_{j,k}$ is the range measurement noise, subscript k means the k_{th} measurement epoch.

Analogously, the impact of the carrier frequency error on velocity error can be written as:

$$\Delta f_{\text{carrier}} = \Delta \boldsymbol{V}_{\text{k}} \cdot \boldsymbol{H}_{\text{j,k}} + c\cdot t_{\text{d,k}} + \eta_{\text{j,k}} \tag{4}$$

Where, the $\Delta f_{carrier}$ is the carrier frequency error, $\Delta \boldsymbol{V}_k$ is the velocity error, c is the speed of the light, $t_{d,k}$ is the clock drift. $\eta_{j,k}$ is the measurement noise, the subscript k is the k_{th} measurement epoch.

Then, the observation equation can be written as:

$$\boldsymbol{z}_k = \begin{bmatrix} \Delta \boldsymbol{\varphi}_k \\ \Delta \boldsymbol{f}_k \end{bmatrix} = h(\Delta \boldsymbol{X}) + v_k = \boldsymbol{H}_k \Delta \boldsymbol{X} + v_k \tag{5}$$

Where, $\boldsymbol{z}_k$ is the observation vector, $\Delta\boldsymbol{\varphi}_k$ is the code phase error obtained from scaled code discriminator, $\Delta\boldsymbol{f}_k$ is the carrier frequency error obtained from scaled carrier frequency discriminator.The details of $\Delta\boldsymbol{\varphi}_k$ and $\Delta\boldsymbol{f}_k$ calculating can be found in references [20-22]. The matrix $\boldsymbol{H}_k$ is composed of Line-Of-Sight vector and it can be written as:

$$\boldsymbol{H}_k=\begin{bmatrix} (LOS_x^1\ LOS_y^1\ LOS_z^1\ -1) & (0\ \ 0\ \ 0) \\ \vdots & \\ (LOS_x^N\ LOS_y^N\ LOS_z^N\ -1) & (0\ \ 0\ \ 0) \\ (0\ \ 0\ \ 0\ \ 0) & (LOS_x^1\ LOS_y^1\ LOS_z^1) \\ \vdots & \\ (0\ \ 0\ \ 0\ \ 0) & (LOS_x^N\ LOS_y^N\ LOS_z^N) \end{bmatrix} \quad (6)$$

Where, $LOS_x^j=\dfrac{x_{j,k}-x_k}{r_{j,k}}$, $LOS_y^j=\dfrac{y_{j,k}-y_k}{r_{j,k}}$, $LOS_y^j=\dfrac{z_{j,k}-z_k}{r_{j,k}}$, the x_k , y_k , z_k is the user's position in ECEF frame at the k_{th} time epoch. $r_{j,k}$ is the distance between j^{th} satellite and the user. $r_{j,k}$ can be calculated using the equation (7).

$$r_{j,k}=\sqrt{(x_{j,k}-(x_k-\delta x))^2+(y_{j,k}-(y_k-\delta y))^2+(z_{j,k}-(z_k-\delta z))^2} \quad (7)$$

III. THE ADAPTIVE ROBUST CUBATURE KALMAN FILTER

This section gives the mathematical equations of the adaptive robust CKF, which heavily references the paper [22]. Considering a discrete nonlinear system:

$$\begin{aligned} \boldsymbol{A}_{k+1}&=f(\boldsymbol{A}_k,k)+\boldsymbol{w}_k \\ \boldsymbol{B}_{k+1}&=h(\boldsymbol{A}_{k+1},k)+\boldsymbol{v}_{k+1} \end{aligned} \quad (8)$$

Where, the state vector $\boldsymbol{A}_k\in\Re^n$, the measurement vector is $\boldsymbol{B}_k\in\Re^m$. The state noise vector is $\boldsymbol{w}_k\in\Re^n$, the measurement noise vector is $\boldsymbol{v}_k\in\Re^m$,The noise vectors $\boldsymbol{w}_k$ and $\boldsymbol{v}_k$ are zero mean Gaussian white sequences with zero cross-correlation with each other.

$$\begin{aligned} \boldsymbol{E}[\boldsymbol{w}_k\boldsymbol{w}_i^T]&=\begin{cases}\boldsymbol{Q}_k, i=k\\ 0, i\neq k\end{cases} \\ \boldsymbol{E}[\boldsymbol{v}_k\boldsymbol{v}_i^T]&=\begin{cases}\boldsymbol{R}_k, i=k\\ 0, i\neq k\end{cases} \\ \boldsymbol{E}[\boldsymbol{w}_k\boldsymbol{v}_i^T]&=0 \end{aligned} \quad (9)$$

Where, $\boldsymbol{Q}_k$ is the state noise covariance matrix, and $\boldsymbol{R}_k$ is the measurement noise covariance matrix.

A. The Cubature Kalman Filter

The CKF implementation and updating steps are given in detail as equation (10) – (23):

First step: initializing the state vector $\hat{\boldsymbol{A}}_{0|0}$ and state covariance matrix $\boldsymbol{P}_{0|0}$;

Second step: CKF Time updating

(1) Factorizing the covariance:

$$\boldsymbol{P}_{k-1|k-1}=\boldsymbol{S}_{k-1}\boldsymbol{S}_{k-1}^T \quad (10)$$

(2) Evaluating the cubature points through the process model:

$$\tilde{\boldsymbol{\chi}}_{k-1}^{(i)}=\hat{\boldsymbol{A}}_{k-1}+\boldsymbol{S}_{k-1}\boldsymbol{\zeta}_i \quad (11)$$

(3) Estimating the propagated cubature points through the process model:

$$\tilde{\boldsymbol{\chi}}_{k|k-1}^{*(i)}=f(\tilde{\boldsymbol{\chi}}_{k-1}^{(i)}) \quad (12)$$

Where the $\boldsymbol{S}_{k-1}$ calculated by the $\boldsymbol{P}_{k-1|k-1}$ using Cholesky decomposing method.

(4) Estimating the predicted mean :

$$\hat{\boldsymbol{A}}_{k|k-1}=\sum_1^{2n}\frac{1}{2n}\tilde{\boldsymbol{\chi}}_{k|k-1}^{*(i)} \quad (13)$$

(5) Estimating the predicted error covariance:

$$\boldsymbol{P}_{k|k-1}=\frac{1}{2n}\sum_1^{2n}\tilde{\boldsymbol{\chi}}_{k|k-1}^{*(i)}(\tilde{\boldsymbol{\chi}}_{k|k-1}^{*(i)})^T-\hat{\boldsymbol{A}}_{k|k-1}\hat{\boldsymbol{A}}_{k|k-1}^T+\boldsymbol{Q}_{k-1} \quad (14)$$

Step Three: Measurement updating

(1) Factorizing the covariance :

$$\boldsymbol{P}_{k|k-1}=\boldsymbol{S}_{k|k-1}\boldsymbol{S}_{k|k-1}^T \quad (15)$$

(2) Evaluating the cubature points:

$$\tilde{\boldsymbol{\chi}}_{k|k-1}^{(i)}=\hat{\boldsymbol{A}}_{k|k-1}+\boldsymbol{S}_{k|k-1}\boldsymbol{\zeta}_i \quad (16)$$

(3) Evaluating the propagated cubature points through observation model:

$$\boldsymbol{B}_{k|k-1}^{(i)}=h(\tilde{\boldsymbol{\chi}}_{k|k-1}^{(i)}) \quad (17)$$

(4) Evaluating the propagated observation:

$$\hat{\boldsymbol{B}}_{k|k-1}=\sum_{i=1}^{2n}\frac{1}{2n}\boldsymbol{B}_{k|k-1}^{(i)} \quad (18)$$

(5) Evaluating the innovation covariance :

$$\boldsymbol{P}_{yy}=\frac{1}{2n}\sum_{i=1}^{2n}[\boldsymbol{B}_{k|k-1}^{(i)}-\hat{\boldsymbol{B}}_{k|k-1}][\boldsymbol{B}_{k|k-1}^{(i)}-\hat{\boldsymbol{B}}_{k|k-1}]^T+\boldsymbol{R}_k \quad (19)$$

(6) Estimating the cross-covariance:

$$\boldsymbol{P}_{xy}=\frac{1}{2n}\sum_{i=1}^{2n}[\tilde{\boldsymbol{\chi}}_{k|k-1}^{(i)}-\hat{\boldsymbol{A}}_{k|k-1}][\boldsymbol{B}_{k|k-1}^{(i)}-\hat{\boldsymbol{A}}_{k|k-1}]^T \quad (20)$$

$$\boldsymbol{K}_k=\boldsymbol{P}_{xy}\boldsymbol{P}_{yy}^{-1} \quad (21)$$

$$\hat{\boldsymbol{A}}_k = \hat{\boldsymbol{A}}_{k|k-1} + \boldsymbol{K}_k[\boldsymbol{B}_k - \hat{\boldsymbol{B}}_{k|k-1}] \quad (22)$$

$$\boldsymbol{P}_k = \boldsymbol{P}_{k|k-1} - \boldsymbol{K}_k \boldsymbol{P}_{yy} \boldsymbol{K}_k^T \quad (23)$$

A. Adaptive Robust Cubature Kalman Filter:

For the adaptive robust CKF (AR-CKF), the details are as equations (24) - (33). The main difference of the CKF and AR-CKF is the changes of the two equations (Eq.14 and Eq.23). The new equation (14) is substituted by the equation (31). For the equation (24), the $\bar{\boldsymbol{P}}_{yy}$ is used to substitute the matrix $\boldsymbol{P}_{yy}$ in the equation (23).

Part1: The Robust Estimation Scheme

The new $\boldsymbol{P}_{yy}$ is defined as $\bar{\boldsymbol{P}}_{yy}$, the details of the calculation is as follows:

$$\bar{\boldsymbol{P}}_{yy} = \frac{1}{2n}\sum_{i=1}^{2n}[\boldsymbol{B}_{k|k-1}^{(i)} - \hat{\boldsymbol{B}}_{k|k-1}][\boldsymbol{B}_{k|k-1}^{(i)} - \hat{\boldsymbol{B}}_{k|k-1}]^T + \bar{\boldsymbol{R}}_k \quad (24)$$

Where $\bar{\boldsymbol{R}}_k$ and $\boldsymbol{R}_k$ are the covariance matrix of the measurement noise, they can be got from inversion of the equivalent weight matrix $\bar{\boldsymbol{P}}$. The $\bar{\boldsymbol{P}}$ is calculated from the robust M estimation.

$$\bar{\boldsymbol{R}}_k = \bar{\boldsymbol{P}}^{-1} \quad (25)$$

Considering the $\bar{p}_{t(ij)}(i, j = 1, 2, ..., n)$ is the matrix elements of the matrix $\bar{\boldsymbol{P}}$ .The details are as follows:

$$\bar{p}_{t(ii)} = \begin{cases} \dfrac{1}{\sigma_{ii}}, & \left|\dfrac{inv_i}{\sigma_{vi}}\right| = \left|inv_i^{est}\right| \le k \\ \dfrac{k}{\sigma_{ii}\left|inv_i^{est}\right|} & \left|inv_i^{est}\right| > k \end{cases} \quad (26)$$

$$\bar{p}_{t(ij)} = \begin{cases} \dfrac{1}{\sigma_{ij}}, & \left|inv_i^{est}\right| \le k, and \left|inv_j^{est}\right| \le k \\ \dfrac{k}{\sigma_{ij} \cdot \max\{\left|inv_i^{est}\right|, \left|inv_j^{est}\right|\}}, & \left|inv_i^{est}\right| > k, or \left|inv_j^{est}\right| > k \end{cases} \quad (27)$$

Where the σ_{ii} is the element on the diagonal of the matrix $\boldsymbol{R}_k$, σ_{ij} is the non-diagonal elements of the matrix $\boldsymbol{R}_k$. inv_i is the residual component of observation measurements and the inv_i^{est} is the standard residual component. Residual component equation is as Equ. (28).

$$inv_i^{est} = \frac{inv_i}{\sigma_{vi}} \quad (28)$$

$$\sigma_{vi} = (\boldsymbol{P}_{yy,k|k-1})_{ii} \quad (29)$$

Part2. The Scheme of the Adaptation

For the filter, the residual component of observation measurements is as following equation (30):

$$inv_i = (\boldsymbol{B}_k - \hat{\boldsymbol{B}}_{k|k-1})_i \quad (30)$$

The key of the adaptive tuning method is to use the adaptive factor α_k to correct formula (14), the corrected formula is equation (31).

$$\bar{\boldsymbol{P}}_{k|k-1} = \frac{1}{\alpha_k}\boldsymbol{P}_{k|k-1} = \frac{1}{\alpha_k}\left(\sum_{i=1}^{2n}\tilde{\boldsymbol{\chi}}_{k|k-1}^{*(i)}(\tilde{\boldsymbol{\chi}}_{k|k-1}^{*(i)})^T - \hat{\boldsymbol{A}}_{k|k-1}\hat{\boldsymbol{A}}_{k|k-1}^T + \boldsymbol{Q}_{k-1}\right) \quad (31)$$

Where, the determination of the adaptive factor α_k is as follows:

$$\alpha_k = \begin{cases} 1 & tr(\hat{\boldsymbol{P}}_{yy,k|k-1}) \le tr(\bar{\boldsymbol{P}}_{yy,k|k-1}) \\ \dfrac{tr(\bar{\boldsymbol{P}}_{yy,k|k-1} - \bar{\boldsymbol{R}}_k)}{tr(\hat{\boldsymbol{P}}_{yy,k|k-1} - \bar{\boldsymbol{R}}_k)}, & tr(\hat{\boldsymbol{P}}_{yy,k|k-1}) > tr(\bar{\boldsymbol{P}}_{yy,k|k-1}) \end{cases} \quad (32)$$

Where the matrix $\bar{\boldsymbol{P}}_{yy,k|k-1}$ calculated from formula (24), $\hat{\boldsymbol{P}}_{yy,k|k-1}$ calculated from formula (33):

$$\hat{\boldsymbol{P}}_{yy,k|k-1} = inv \cdot inv^T \quad (33)$$

IV. SIMULATION AND EXPERIMENT

A software simulation is carried out to evaluate the performance of the AR-CKF in comparison with EKF approach for navigation filter in VTL. The AR-CKF and EKF is implemented in a VTL software in MATLAB. The VTL processes the trajectory IF signal data acquired by an IF data collector from a GPS hardware signal simulator. Table 1 reviews the IF signal parameters including the sampling frequency and immediate frequency. Figure 2 gives the 3-dimension plot of the dynamic trajectory in detail. Considering the VTL computation load and the processing time, the time trajectory time length is approximately 360 seconds. Numbers in the figure 2 refer to different motion tasks (0: straight fly; 1: acceleration; 2: deceleration; 3: up; 4: down; 5: turn right; 6: tune left).

Table 1. Immediate frequency signal parameters

Sampling frequency	Immediate frequency
16.369MHz	3.996MHz

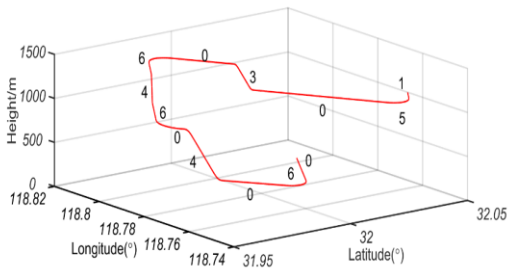

Figure 2 A 3-Dimensional plot of the trajectory and numbers represent the flying tasks.

Two different navigation filters are implemented in simulation including a common EKF and AR-CKF. The two filters are operated with same parameters setting and trajectory plotted in Figure 2. Navigation performance is compared in terms of positing accuracy. Figure 3, Figure 4 and Figure 5 show position errors from the two different navigation filters in ECEF coordinates. In the pictures, the red line represents the EKF navigation filter position errors, blue line represents the AR-CKF navigation filter position errors.

In can be seen that both navigation filters can converge the position errors. AR-CKF has better position accuracy through position errors curves. The statistic results of position errors are as Table 2, in which square mean root errors and mean errors are selected for comparison. The AR-CKF has a great improvement against EKF in terms RMSE of position.

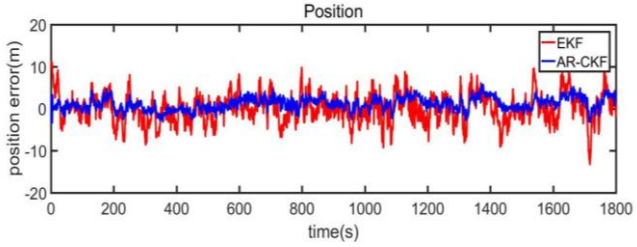

Figure 3. Position error X

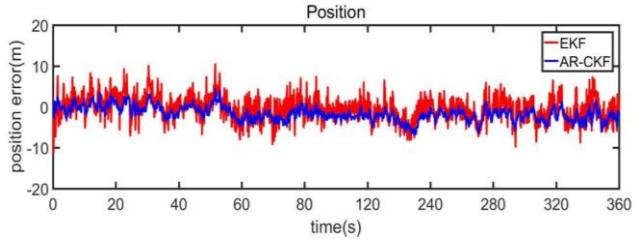

Figure 4. Position error Y

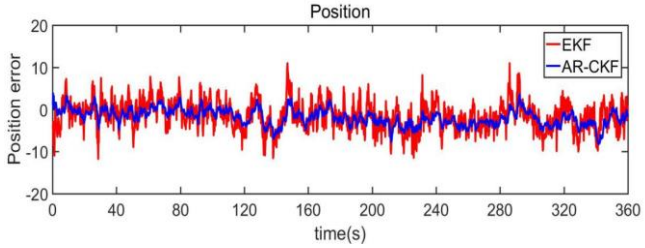

Figure 5. Position error Y

Table 2. Position Errors Comparison

	EKF		AR-CKF	
	MEAN	**RMSE**	**MEAN**	**RMSE**
Position error X(m)	2.71	4.51	1.54	1.26
Position error Y(m)	2.68	4.23	1.48	1.17
Position error Z(m)	2.95	4.87	1.72	1.41

V. CONCLUSIONS

In this paper, an adaptive robust cubature Kalman filter is constructed and applied in VTL to deal with the navigation filter nonlinearity and measurement noise uncertainty. CKF is employed for addressing nonlinear model of the VTL observation data and robust estimator is utilized to address measurement noise uncertainty. Then, a common EKF and the AR-CKF are implemented in a GPS VTL software. Position accuracy is carried out using a dynamic trajectory. Results show that AR-CKF is able to improve the position accuracy.

VI. CONCLUSION

A conclusion section is not required. Although a conclusion may review the main points of the paper, do not replicate the abstract as the conclusion. A conclusion might elaborate on the importance of the work or suggest applications and extensions.

REFERENCES

[1] Kaplan, E.; Hegarty, C. Understanding GPS: Principles ans Applications, 2nd ed; Artech House: Boston, MA, USA, 2006, pp.3-30.
[2] Mirsa, P.; Enge, P. Global Positioning System: Signals, Measuments, and Performance, 2nd ed.; Ganag-Jamuna Press: Lincoln, MA, USA, 2006; pp. 1-20.
[3] Sun Z, Wang X, Feng S, et al. Design of an adaptive GPS vector tracking loop with the detection and isolation of contaminated channels [J]. GPS solutions, 2017, 21(2): 701-713.
[4] Spilker, J.J. Vector Delay Lock Loop Processing of Radiolocation Transmitter Signals. US Patent 5398034, 13 October 1994.
[5] Lashley, M.; Bevly, D.M.; Hohn Y.Hung. A Valid Comparison of Vector and Scalar Tracking Loops. PLANS 2010: 464-474.
[6] Lashley, M.; Bevly, D.M.; Hung, J.Y. Performance analysis of vector tracking algorithms for weak GPS signals in high dynamics. Sel. Top. Signal Process. IEEE J. 2009, 4, 661–673.
[7] Lashely, M.; Bevly, D.M. Analysis of Discriminator Based Vector Tracking Algorithms. In Proceedings of the Institute of Navigation (NTM), San Diego, CA, USA, 22–24 January 2007.
[8] Zhao, S.H.; Lu, M.Q.; Feng, Z.M. Implementation and Performance Assessment of a Vector Tracking Method Based on a Software GPS Receiver. Journal of Navigation. 2011, 641, 151-161.
[9] Zhao, S.H.; D. Akos. “An Open Source GPS/GNSS Vector Tracking Loop – Implementation, Filter Tuning, and Results”, ION ITM 2011.
[10] Luo, Yong, et al. "Double-filter model with modified Kalman filter for baseband signal pre-processing with application to ultra-tight GPS/INS integration." GPS solutions 16.4 (2012): 463-476.
[11] Wu, Mouyan, et al. "An adaptive deep-coupled GNSS/INS navigation system with hybrid pre-filter processing." Measurement Science and Technology 29.2 (2018): 025103.
[12] Xiyuan Chen, et al.,” Performance Enhancement for GPS Vector-Tracking Loop Utilizing an Adaptive Iterated Extended Kalman Filter”. Sensors, Vol 14, 2014, pp.23630.
[13] Chien-Hao T, Lin S F, Dah-Jing J. “Fuzzy Adaptive Cubature Kalman Filter for Integrated Navigation Systems [J].” Sensors, 2016, 16(8):1167.
[14] Zhao Y. “Performance evaluation of Cubature Kalman filter in a GPS/IMU tightly-coupled navigation system [J].” Signal Processing, 2016, 119(C):67-79.
[15] Zhao Y. “Cubature + Extended Hybrid Kalman Filtering Method and Its Application in PPP/IMU Tightly Coupled Navigation Systems [J].” IEEE Sensors Journal, 2015, 15(12):1-1.
[16] Jwo, Dah-Jing, et al. "Performance enhancement for ultra-tight GPS/INS integration using a fuzzy adaptive strong tracking unscented Kalman filter." Nonlinear Dynamics 73.1-2 (2013): 377-395.
[17] Chang, Guobin. "Loosely coupled INS/GPS integration with constant lever arm using marginal unscented Kalman filter." The Journal of Navigation 67.3 (2014): 419-436.
[18] Liu, Yahui, et al. "An innovative information fusion method with adaptive Kalman filter for integrated INS/GPS navigation of autonomous vehicles." Mechanical Systems and Signal Processing 100 (2018): 605-616.
[19] Zhao, Sihao, Mingquan Lu, and Zhenming Feng. "Implementation and performance assessment of a vector tracking method based on a software GPS receiver." The Journal of Navigation 64.S1 (2011): S151-S161.
[20] Jiang C, Chen S, Chen Y, et al. Performance Analysis of GNSS Vector Tracking Loop Based GNSS/CSAC Integrated Navigation System [J]. Journal of Aeronautics, Astronautics and Aviation, 2017, 49(4): 289-297.
[21] Jiang, Changhui, et al. "Performance improvement of GPS/SINS ultra-tightly integrated navigation system utilizing a robust Cubature Kalman Filter." Journal of Aeronautics, Astronautics and Aviation 49.1 (2017): 49-55.

Boya Zhang, a postgraduate of School of Automation, Nanjing University of Science and Technology, Nanjing,China.Research on integrated navigatioin.

Shuai Chen, an associate professor of School of Automation, Nanjing University of Science and Techology, Nanjing, China, Research on integrated navigation.

Xiaohan Zhu, a postgraduate of School of Automation, Nanjing University of Science and Technology, Nanjing, China. Research on integrated navigation.